VSB Modified Duobinary PAM4 Signal Transmission in an IM/DD System With Mitigated Image Interference

Jingchi Li, Shaohua An, Qingming Zhu, Xingfeng Li, and Yikai Su, *Senior Member, IEEE*

***Abstract*— We experimentally demonstrate a 56-Gb/s vestigial sideband (VSB) modified duobinary (MDB) 4-level pulse amplitude modulation (PAM4) signal transmission over an 80-km single-mode fiber (SMF) in an intensity-modulation and direct-detection (IM/DD) system without optical dispersion compensation. Compared to the conventional PAM4 signal without pulse shaping, the MDB PAM4 signal exhibits a higher spectral efficiency (SE) due to the modified duobinary precoding. Moreover, if VSB modulation is employed to mitigate the chromatic dispersion (CD)-induced power fading, the VSB MDB PAM4 signal suffers less image interference resulting from VSB filtering and direct detection (DD), thanks to its lower components at the carrier frequency. A proof-of-concept experiment is performed, in which the performances of the conventional VSB PAM4 signal, the VSB Nyquist PAM4 signal, and the VSB MDB PAM4 signal are investigated and compared comprehensively. The experimental results show that only the VSB MDB PAM4 signal can reach the bit error ratio (BER) below the 20% soft-decision forward error correction (SD-FEC) threshold of 2.4×10^{-2} at the 56-Gb/s rate after the 80-km SMF transmission, due to the mitigated image interference.**

***Index Terms*— Intensity modulation, modified duobinary, PAM4, VSB.**

I. Introduction

DRIVEN by the emerging applications such as cloud network and real-time service, the transmission capacity demands in metro and data center interconnections are growing rapidly [1]. Systems based on intensity-modulation and direct-detection (IM/DD) are preferred for these scenarios due to low costs, low power consumptions, and simple implementations [2]. Meanwhile, various advanced modulation formats have been used in current IM/DD systems such as 4-level pulse amplitude modulation (PAM4), carrier-less amplitude and phase modulation (CAP), and discrete multi-tone modulation (DMT) [2]. Among these schemes, PAM4 is an attractive modulation format because it has become the standard modulation scheme for the 400 GE [3]. However, when scaling the system to a higher data rate and a longer transmission distance, the chromatic dispersion (CD)-induced power fading is a main performance-limiting factor. It is known that single sideband (SSB) modulation is an effective method to overcome the CD limitation by removing the redundant sideband of a double sideband (DSB) signal [4]. In general, an SSB signal can be generated by optical or digital means [5]–[9]. Among these schemes, the approach based on optical SSB filtering provides an economical solution with one digital-to-analog converter (DAC) and a low-cost intensity modulator (IM), which is often referred to as vestigial sideband (VSB) modulation. The VSB scheme leads to a non-ideal SSB spectrum due to the limited sharpness of the passband edge though. As a result, the image interference caused by the VSB filtering and DD greatly degrades the system performance [9]–[11]. To mitigate the image interference, an equalization or an interference cancellation scheme is typically used in the receiver, but at the expense of an increased computational complexity [12], [13].

In order to reduce the image interference while retaining a low computational complexity, here we propose a VSB modified duobinary (MDB) PAM4 format. The MDB PAM4 signal features a cosine spectral profile that decays to zero at its carrier frequency, i.e., the low-frequency components of the MDB PAM4 signal are weak. Therefore, if the MDB PAM4 signal is VSB filtered and square-law detected, it suffers less image interference resulting from the VSB filtering and DD due to its spectral characteristic. However, the conventional PAM4 signal, the Nyquist PAM4 signal, and the duobinary (DB) PAM4 signal all have strong components at the carrier frequencies. In such cases, the VSB filtering induces severe image interference after the square-law detection in the presence of CD, since strong low-frequency components in the other sideband cause destructive interference to the desired sideband. On the other hand, the proposed VSB MDB PAM4 signal can achieve better BER performance, due to the mitigated image interference. The MDB signal can be generated by setting the modulator bias at its transmission quadrature or null point. Since a VSB signal is directly detected based on self-beating, a strong optical carrier is required and thus the modulator is biased at the quadrature point in the experiment [14].

In this letter, we experimentally demonstrate a 56-Gb/s VSB MDB PAM4 signal transmission over an 80-km single-mode fiber (SMF) in an IM/DD system. The optical VSB modulation can overcome the CD limitation in an IM/DD system, and the proposed VSB MDB PAM4 format mitigates the image interference caused by the VSB filtering and DD. Therefore,

Manuscript received December 24, 2019; revised January 21, 2020; accepted February 19, 2020. Date of publication February 24, 2020; date of current version March 3, 2020. This work was supported in part by the National Natural Science Foundation of China under Grant 61835008 and in part by the Science and Technology Commission of Shanghai Municipality under Grant 17500710900. *(Corresponding author: Yikai Su.)*

The authors are with the State Key Laboratory of Advanced Optical Communication Systems and Networks, Department of Electronic Engineering, Shanghai Jiao Tong University, Shanghai 200240, China (e-mail: jingchi_lee@sjtu.edu.cn; shaohuaan@sjtu.edu.cn; zhuqmg@sjtu.edu.cn; lxfshu@163.com; yikaisu@sjtu.edu.cn).

Color versions of one or more of the figures in this letter are available online at http://ieeexplore.ieee.org.

Digital Object Identifier 10.1109/LPT.2020.2975839

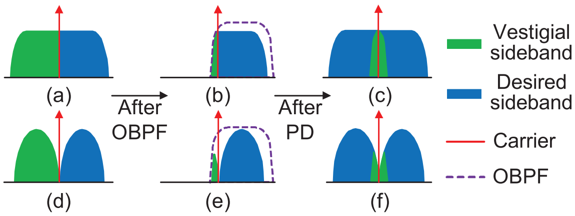

Fig. 1. Spectra at different stages for the VSB Nyquist PAM4 signal and the VSB MDB PAM4 signal, respectively.

a low-complexity equalization method, e.g., a least mean square (LMS)-based linear feed-forward equalization (FFE), can be used at the receiver side. Finally, we compare the performances of a conventional VSB PAM4 signal, a VSB Nyquist PAM4 signal, and the VSB MDB PAM4 signal after the 80-km SMF transmissions. Only the VSB MDB PAM4 signal can reach the bit error ratio (BER) threshold of 2.4×10^{-2}.

II. Operation Principle

In order to avoid the power fading problem, a DSB signal with a Hermitian symmetric Fourier transform can be filtered to obtain a SSB signal. However, the imperfect optical filtering leads to a VSB signal, suffering severe image interference after DD [9]–[13]. The motivation for proposing the VSB MDB PAM4 format is discussed using Fig. 1, which shows the spectra at different stages for the VSB Nyquist PAM4 signal and the VSB MDB PAM4 signal, respectively. The red arrow represents the carrier component. Fig. 1(a) and Fig. 1(d) illustrate the optical spectra of the DSB Nyquist PAM4 signal and the DSB MDB PAM4 signal before OBPF, respectively. One can observe that the DSB MDB PAM4 signal has a cosine spectrum that decays to zero at the carrier frequency, leading to weak low-frequency components. After the OBPF, the limited sharpness of the optical filter results in a VSB signal, and the square-law detection of the photodetector (PD) leads to the superposition between two sidebands. The superposition is useful in the absence of CD, whereas it becomes the interference through a dispersive channel. However, compared to the VSB Nyquist PAM4 signal, the VSB MDB PAM4 signal suffers less interference due to its weaker low-frequency components, thus can improve the quality of the desired signal as well as the BER performance.

The MDB signaling is a partial response signaling (PRS) which can relax the bandwidth requirement and improve the spectral efficiency (SE) by exploiting controlled intersymbol interference (ISI). In a system using the MDB signaling, if a_k is the initial PAM4 sequence, the MDB PAM4 signal can be generated as follows [15], [16]:

$$c_k = a_k - a_{k-2}, \tag{1}$$

where c_k represents the MDB-coded sequence. Generally, to avoid error propagation caused by the MDB-coding, pre-coding is required prior to MDB-coding [15], [16]:

$$b_k = (a_k + b_{k-2}) \bmod 4, \tag{2}$$

$$c_k = b_k - b_{k-2}, \tag{3}$$

where b_k is the pre-coded sequence. After pre-coding and MDB-coding, a four-level PAM4 signal is converted to a seven-level MDB PAM4 signal. As a result, a seven-level hard decision operation and a modulo-4 operation are necessary at the receiver side to recover the initial PAM4 signal [15], [16]:

$$d_k = (c_k) \bmod 4, \tag{4}$$

where d_k is the decoded sequence. Thus, the transmitted symbol is only decided by the currently received symbol, and the error propagation is removed.

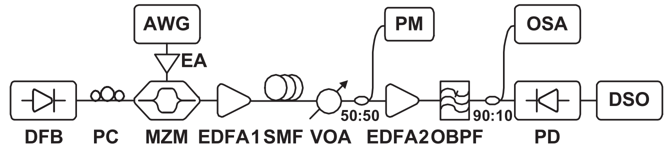

Fig. 2. Experimental setup. PM: power meter.

III. Experimental Setup

The experimental setup of the VSB MDB PAM4 system is shown in Fig. 2. At the transmitter, a 28-GBaud PAM4 signal is generated by an arbitrary waveform generator (AWG) (Keysight M8195A), operating at a sampling rate of 56 GSa/s. The output of the AWG is first amplified by an electrical amplifier (EA) and then drives a 25-GHz IM with a quadrature bias condition. In the experiment, we optimized the optical modulation index (OMI) through changing the amplitude of the signal output from the AWG, and carefully adjusted the bias of the IM at the quadrature. A distributed feedback laser (DFB) is used as the light source, followed by a polarization controller (PC) to align the polarization state of the optical signal and the IM. Then, a continuous wave light at ~1550.65 nm from the DFB laser is fed into the IM to generate the optical signal, which is then amplified by an erbium-doped fiber amplifier (EDFA) before launched into an 80-km SSMF link. At the receiver, the received optical power (ROP) is adjusted using a variable optical attenuator (VOA), followed by a second EDFA to boost the signal. Then, an OBPF (EXFO XTM-50) with an edge roll-off of 800 dB/nm is applied to generate the optical SSB signal and filter out the out-of-band noise simultaneously; this saves one EDFA compared to the transmitter side filtering. The 3-dB bandwidth of the OBPF is 75 GHz. The received optical signal is converted to an electrical signal by a 40-GHz PD and then captured by an 80-GSa/s digital storage oscilloscope (DSO) (LeCroy 36Zi-A). A 90:10 optical splitter is employed after the OBPF, tapping out 10% of the optical power in order to monitor the optical spectrum using an optical spectrum analyzer (OSA) (APEX AP2040C). Finally, the signal is processed by offline digital signal processing (DSP).

Fig. 3 presents the DSP flow charts. At the transmitter, a pseudo-random bit sequence (PRBS) is mapped to the PAM4 signal firstly, and a synchronization sequence is added. Then, different signal processing schemes are implemented for different formats. For the conventional PAM4 signal, the signal is resampled to 56 GSa/s by a zero-order holding operation and then loaded to the AWG. When implementing the Nyquist PAM4 signal, the signal is up-sampled, followed by a raise cosine (RC) filter with a roll-off factor of 0.01. The resulting signal is resampled to 56 GSa/s and loaded to the AWG. As for

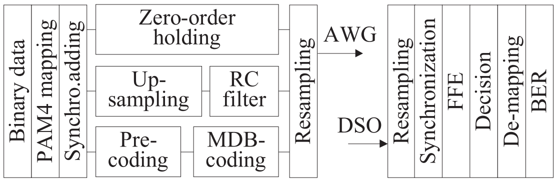

Fig. 3. DSP flow charts.

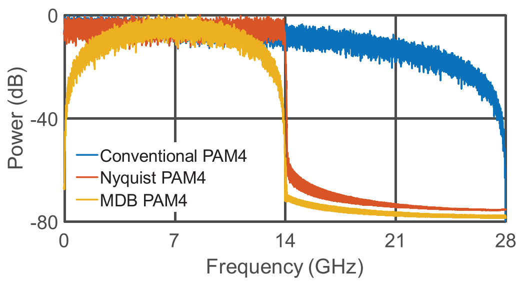

Fig. 4. Electrical spectra of the signals generated offline and loaded to the AWG.

the MDB PAM4 signal, the signal is pre-coded, MDB-coded, and resampled to 56 GSa/s to align the sampling rate of the AWG. The electrical spectra of the three signals generated offline and loaded to the AWG are provided in Fig.4. The bandwidth of the MDB PAM4 signal is half of the baud rate, due to the MDB precoding. At the receiver, resampling and synchronization are firstly implemented for all three signals, followed by a LMS based linear FFE to mitigate the system impairment. Afterwards, a traditional four level hard decision is employed for the conventional VSB PAM4 signal and the VSB Nyquist PAM4 signal, whereas seven level hard decision and the modulo-4 operation are needed for the VSB MDB PAM4 signal. Finally, after PAM de-mapping, BER calculation is performed to evaluate the system performance.

IV. Experimental Results

The BER results in the OBTB case are shown in Fig. 5. Note that the amplitude of the signal output from the AWG was optimized according to the BER for each signal at different offset frequencies. The offset frequency is defined as the difference between the optical carrier frequency and the −3-dB frequency of the OBPF, as indicated in Fig. 6(a) with a red arrow. In the experiment, different offset frequencies were obtained by adjusting the optical carrier frequency, with the fixed center frequency and the bandwidth of the OBPF. The signals are the DSB signals at the offset frequency near 28 GHz, and the MDB PAM4 signal exhibits the highest BER, since it possesses more signal levels after the MDB precoding. As the offset frequency decreases, a DSB signal is filtered to be a VSB signal which introduces a theoretical 3-dB penalty, whereas the signal-signal beat interference (SSBI) and nonlinear behaviors of the optoelectronic components and the fiber transmission also limit the system performance. Thus, the BER increases about two orders of magnitude for all the three signals. When the offset frequency decreases to a few GHz frequency, both the carrier and the desired sideband of the signal suffer from the power attenuation due to the limited sharpness of the OBPF band edge, leading to high BERs for all the three signals.

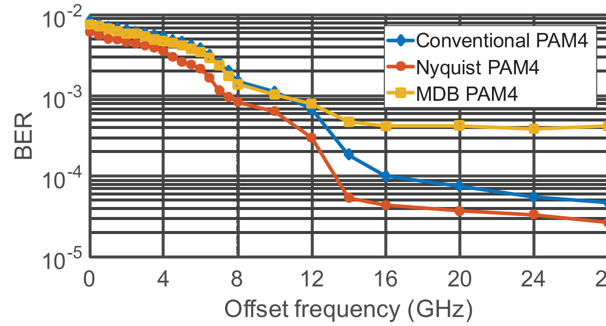

Fig. 5. BER versus offset frequency in the OBTB case.

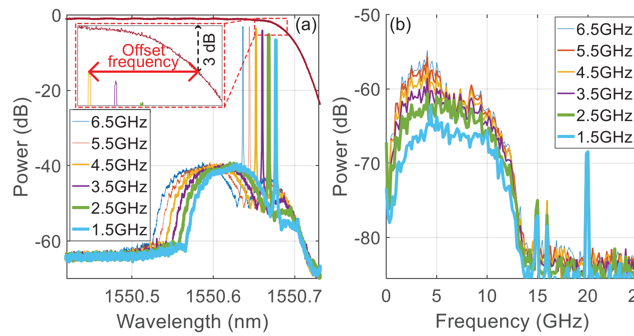

Fig. 6. (a) Optical spectra at the output of the OBPF. (b) Electrical spectra at the receiver.

After the 80-km transmission, the optical spectra of the VSB MDB PAM4 signal under different offset frequencies are shown in Fig. 6(a), measured by the OSA with a resolution bandwidth of 1.12-pm. The carrier-to-signal power ratio (CSPR) at 3.5-GHz offset frequency is measured to be 17.7 dB. Fig. 6(b) depicts the received electrical spectra correspondingly. The frequency components near 15 GHz and 20 GHz are the clock leakages of the DAC of the AWG and the analog-to-digital converter (ADC) of the DSO. As shown in Fig. 6(b), the power fading is obvious for the large offset frequency value, and reducing the offset frequency can mitigate this effect. Fig. 7 shows the BER results of the three formats under different offset frequencies after the 80-km transmission. As shown, the VSB MDB PAM4 signal achieves the best BER performance compared to other signals, since the image interference resulting from the VSB filtering and DD is mitigated. Due to the limited sharpness of the OBPF band edge, the bandwidth of the undesired sideband is larger than the offset frequency. Thus, at 0-GHz offset frequency, the signal is still a VSB signal and the detected signal suffers from the power fading. Only the VSB MDB PAM4 signal can reach the BER of the 20% SD-FEC after the fiber transmission. Note that only FFE is employed to mitigate the linear impairments in the experiments with the nonlinearities uncompensated, and this is the main reason for the relative poor opening in the upper parts of the eye diagrams of the insets. The SSBI cancellation scheme and nonlinear equalizer can indeed improve the performance, but they are not employed in this work, since it is a proof-of-concept experiment and we want to study the performance of the VSB signal with a low computational complexity. Moreover, we can observe that the optimum offset frequency is 3.5 GHz

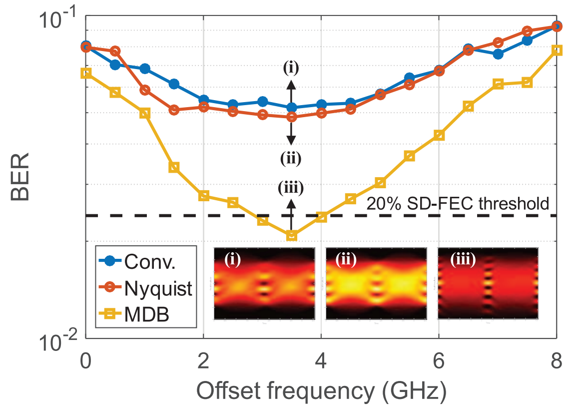

Fig. 7. BER versus offset frequency after the 80-km transmission. Insets (i-iii): eye diagrams at the 3.5-GHz offset frequency for the convention VSB PAM4, the VSB Nyquist PAM4, and the VSB MDB PAM4, respectively.

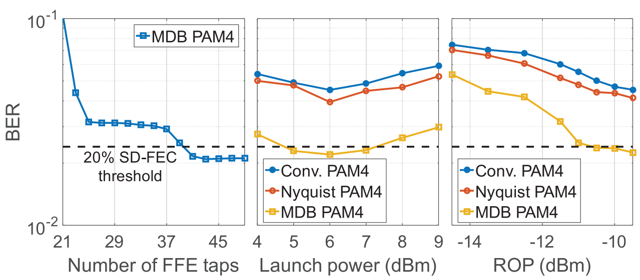

Fig. 8. Transmission performances. (a) BER versus number of FFE taps, (b) BER versus launch power, and (c) BER versus ROP, at the optimal offset frequency.

for all the three signals after the fiber transmission. If the offset frequency is larger than the optimum offset frequency, severe dispersion induced power fading limits the performance. On the other hand, an offset frequency lower than the optimum value leads to an increased BER. This is because reducing the offset frequency not only suppresses the vestigial sideband signal but also results in a power attenuation of the desired sideband and the carrier, due to the limited sharpness of the OBPF band edge.

Fig. 8(a) plots the BER curve as a function of number of FFE taps after the 80-km transmission. The step behavior may be attributed to the choice of the step size, which is set to be 0.0001 in our experiment [17]. A larger tap number of FFE reduces the BER effectively. However, when the number of the FFE taps increases beyond 43, the extra taps do not improve the system performance significantly. Therefore, the number of the FFE taps is set to 43 in our experiment, considering the trade-off between the computational complexity and the system performance. Fig. 8(b) provides the BER results with different launch powers at the optimum offset frequency after the 80-km transmission. All the three signals have a same optimum launch power of 6 dBm. Fig. 8(c) shows the BER curves as a function of received optical power (ROP) at the optimum offset frequency after the 80-km transmission. For the proposed VSB MDB PAM4 signal, the minimum required optical power to reach the 20% SD-FEC threshold is -10.6 dBm. On the other hand, the VSB Nyquist PAM4 signal achieves a slightly better performance compared to the conventional VSB PAM4 signal, due to the narrower bandwidth after the Nyquist pulse shaping.

V. Conclusion

In this paper, we propose a VSB MDB PAM4 format to reduce the image interference caused by the VSB filtering and DD. The VSB MDB PAM4 signal features a spectral profile that decays to zero at the carrier frequency, which can mitigate the image interference. Moreover, we compare the performances of the conventional VSB PAM4 signal, the VSB Nyquist PAM4 signal, and the VSB MDB PAM4 signal after the 80-km SMF transmissions. Only the 56-Gb/s VSB MDB PAM4 signal can reach the BER below the 20% SD-FEC threshold of 2.4×10^{-2} with a LMS based linear FFE at the receiver side. For the first time to the best of our knowledge, the VSB MDB PAM4 format is proposed and experimentally demonstrated in an IM/DD system without optical dispersion compensation.

References

[1] Cisco. (2018). *Cisco Global Cloud Index: Forecast and Methodology, 2016–2021 White Paper*. [Online]. Available: https://www.cisco.com/c/en/us/solutions/collateral/service-provider/global-cloud-index-gci/white-paper-c11-738085.pdf

[2] K. Zhong *et al.*, "Experimental study of PAM-4, CAP-16, and DMT for 100 Gb/s short reach optical transmission systems," *Opt. Express*, vol. 23, no. 2, pp. 1176–1189, Jan. 2015.

[3] *Draft Standard for Ethernet Amendment: Media Access Control Parameters, Physical Layers and Management Parameters for 200 Gb/s and 400 Gb/s, Operation*, IEEE Standard P802.3bs/D2.1, Oct. 2016.

[4] S. An, Q. Zhu, J. Li, and Y. Su, "Generation and transmission of SSB-PAM4 signal with a DSP-free phase alignment scheme," in *Proc. ACP*, 2018, pp. 1–3, Paper Su2A.132.

[5] M. Sieben, J. Conradi, and D. E. Dodds, "Optical single sideband transmission at 10 Gb/s using only electrical dispersion compensation," *J. Lightw. Technol.*, vol. 17, no. 10, pp. 1742–1749, Oct. 1999.

[6] M. Zhu *et al.*, "Optical single side-band Nyquist PAM-4 transmission using dual-drive MZM modulation and direct detection," *Opt. Express*, vol. 26, no. 6, pp. 6629–6638, Mar. 2018.

[7] Z. Li *et al.*, "Spectrally efficient 168 Gb/s/λ WDM 64-QAM single-sideband nyquist-subcarrier modulation with Kramers–Kronig direct-detection receivers," *J. Lightw. Technol.*, vol. 36, no. 6, pp. 1340–1346, Mar. 15, 2018.

[8] S. T. Le *et al.*, "1.72-Tb/s virtual-carrier-assisted direct-detection transmission over 200 km," *J. Lightw. Technol.*, vol. 36, no. 6, pp. 1347–1353, Mar. 15, 2018.

[9] H.-Y. Chen, N. Kaneda, J. Lee, J. Chen, and Y.-K. Chen, "Optical filter requirements in an EML-based single-sideband PAM4 intensity-modulation and direct-detection transmission system," *Opt. Express*, vol. 25, no. 6, pp. 5852–5860, Mar. 2017.

[10] H.-Y. Chen, J. Lee, N. Kaneda, J. Chen, and Y.-K. Chen, "Comparison of VSB PAM4 and OOK signal in an EML-based 80-km transmission system," *IEEE Photon. Technol. Lett.*, vol. 29, no. 23, pp. 2063–2066, Dec. 1, 2017.

[11] Z. Xing *et al.*, "100 Gb/s PAM4 transmission system for datacenter interconnects using a SiP ME-MZM based DAC-less transmitter and a VSB self-coherent receiver," *Opt. Express*, vol. 26, no. 18, pp. 23969–23979, Aug. 2018.

[12] S. Randel, D. Pilori, S. Chandrasekhar, G. Raybon, and P. Winzer, "100-Gb/s discrete-multitone transmission over 80-km SSMF using single-sideband modulation with novel interference-cancellation scheme," in *Proc. ECOC*, 2015, pp. 1–3.

[13] J. Lee, N. Kaneda, and Y. K. Chen, "112-Gbit/s intensity-modulated direct-detect vestigial-sideband PAM4 transmission over an 80-km SSMF link," in *Proc. ECOC*, 2016, pp. 1–3.

[14] Q. Zhang *et al.*, "Single-lane 180 Gb/s SSB-Duobinary-PAM-4 signal transmission over 13 km SSMF," in *Proc. OFC*, 2017, pp. 1–3, Paper Tu2D.2.

[15] S. Walklin and J. Conradi, "Multilevel signaling for increasing the reach of 10 Gb/s lightwave systems," *J. Lightw. Technol.*, vol. 17, no. 11, pp. 2235–2248, Nov. 1999.

[16] A. Lender, "Correlative level coding for binary-data transmission," *IEEE Spectr.*, vol. 3, no. 2, pp. 104–115, Feb. 1966.

[17] R. D. Gitlin and S. B. Weinstein, "On the required tap-weight precision for digitally implemented, adaptive, mean-squared equalizers," *Bell Syst. Tech. J.*, vol. 58, no. 2, pp. 301–321, Jul. 2013.